Flutter in High Aspect Ratio Wings using Numerical Continuation

A.J. Eaton[1], C. Howcroft[1], S.A. Neild[1], M.H. Lowenberg[1], J.E. Cooper[1], E. Coetzee[2]

[1]University of Bristol
[2]Airbus Operations Ltd.
andrew.eaton@bristol.ac.uk

September 19, 2016

Abstract

This paper presents a study into the occurrence of aeroelastic flutter in a high aspect ratio wing using numerical continuation and a geometrically nonlinear beam model. This beam model comprises a continuous, assumed-shape formulation and is coupled with strip theory aerodynamics. Out-of-plane, in-plane and torsional stiffness properties are varied and their influences on the flutter point are observed. A nonlinear lift curve is incorporated so as to illustrate the influence of stall effects. The occurrence of a subcritical Hopf bifurcation is also demonstrated, indicating the possibility of oscillation at airspeeds below the flutter velocity, given a sufficient wing perturbation.

I. Introduction

High aspect ratio wing designs are currently of significant interest in the aerospace industry, due to the reduction in vortex-induced drag they provide [1]. Such designs are inherently more flexible and can be subject to large deformations during flight, leading to the re-orientation of aerodynamic force vectors, effective tip shortening (see Figure 1) and stall effects [2]. Consequently, the linear approximations suitable for more rigid wings are no longer appropriate and treatment of these configurations must fully account for nonlinear behaviour. Fully understanding the aeroelastic properties of these designs is vital, as the flutter stability boundaries and gust/manoeuvre responses are likely to differ from conventional aircraft configurations.

Flutter is a dynamic aeroelastic instability classically defined as the condition where small disturbances to a stable wing do not decay to a steady state. The presence of limit cycle oscillations (LCOs) typically bound this instability, limiting what would otherwise be exponential growth. In this paper, the flutter velocity (denoted by V_F) is defined as the lowest airspeed at which this type of behaviour occurs, i.e. the airspeed at which static stability is lost and any perturbation results in an oscillatory response.

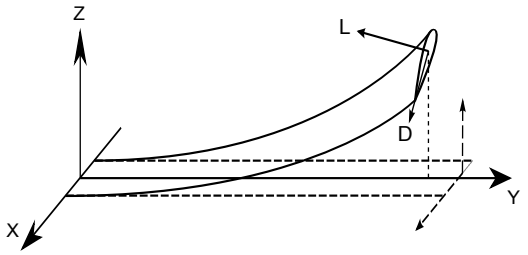

Figure 1: *High aspect ratio wing deformation showing re-orientation of aerodynamic forces and effective tip shortening.*

The aeroelastic characteristics of high aspect ratio wings has been the subject of numerous studies [3]. Patil et al. [5] used a geometrically exact intrinsic nonlinear beam formulation cou-

pled with finite-state unsteady aerodynamics (with static stall) and observed that flutter velocity decreased as the wing became more statically deformed. In this case, the deformed shape was produced using a specified tip load. Tang and Dowell [6] used similar beam equations with 3rd order geometric nonlinear terms removed; deformed wing shapes in this study were achieved by several means: a vertical tip load, a manufactured wing curvature and a nonzero angle of attack. Flutter velocities are seen to decrease for all sources of deformation.

In most studies, the velocity at which flutter occurs is typically determined via extensive use of numerical integration; airspeed is gradually increased and the long term response is investigated for periodic behaviour. A more direct approach is to use a technique common in nonlinear dynamics analysis called numerical continuation; this method is an algorithmic procedure for finding the steady states of a parameterised system of first order ODEs, such as

$$\dot{x} = F(x, p) \tag{1}$$

where $x \in \mathbb{R}^n$ and $p \in \mathbb{R}^m$ correspond to the states and parameters of the system respectively. The method effectively solves for the implicit curve $F(x, p) = 0$ and thus illustrates how equilibria (e.g. steady states) vary as system parameters change. Periodic orbits may also be computed using a variation of this technique. Additional constraints are imposed in order to detect bifurcations (i.e. topological changes in the dynamical behaviour) that occur when parameters cross certain thresholds. The exactness and efficiency of this method provides a distinct advantage over other techniques that rely on exhaustive numerical integration.

Numerical continuation has historically seen use in a few aerospace applications, for example in the investigation of closed loop flight controls of fighter aircraft and landing gear shimmy of commercial aircraft. A useful industrial perspective of the technique is provided by Sharma et al [8].

The type of bifurcation associated with the onset of nonlinear flutter is the Hopf bifurcation. This bifurcation typically changes the stability of a steady state and produces some kind of LCO response. Such a bifurcation occurs when a complex conjugate pair of eigenvalues of the system Jacobian crosses the imaginary axis; in an aeroelastic system this corresponds to the point where the damping of a mode of vibration becomes zero.

This paper uses numerical continuation to investigate the relationship between the occurance of flutter and the stiffness properties of a high aspect ratio, rectangular High Altitude, High Endurance (HALE) wing. Specifically, it investigates how the value of V_F changes when stiffnesses are varied about nominal values. The study considers both linear and nonlinear lift profiles so as to investigate the influence of stall effects. Wing deformation is acheived by using a nonzero root angle of attack (α_0) and by taking account of gravitational forces.

II. Model Description

The aeroelastic model used in this study is an energy-based, reduced order structural formulation coupled with strip theory aerodynamics, as presented by Howcroft et al. [2][4]. The deformation of the wing is expressed as a sum of weighted continuous shape functions; these describe the orientation of local span-wise reference vectors that remain aligned to the wing as it undergoes deflection. Such an approach is well suited to the formulation shown in Equation (1). Three degrees of motion are modelled: out-of-plane (flapwise) bending, in-plane (chordwise) bending and spanwise twist. The wing considered in this study is a HALE wing with constant spanwise properties (see Table 1), as used in [5]. Gravitational effects are assumed to be present (unless otherwise stated) and structural damping is assumed proportional to stiffness properties. For the analyses in this paper, a total of 12 Chebyshev polynomials are used as shape functions.

Aerodynamic forces are accounted for by use of a two dimensional, strip theory approach and are modelled to follow the deformed wing. Lift coefficient (C_L) is a function of local angle of attack (α) and is modelling using two differ-

Table 1: *Nominal wing parameters*

Name	
Name	Value
Half-span	16 m
Chord	1 m
Mass	0.75 kgm^{-1}
Moment of inertia	0.1 kgm
Elastic axis	50% chord
Centre of gravity	50% chord
Out-of-plane stiffness (EI_1)	2 x 10^4 Nm^2
In-plane stiffness (EI_2)	4 x 10^6 Nm^2
Torsional stiffness (GJ)	1 x 10^4 Nm^2
Air density	0.0881 kg/m^3
Root angle of attack (α_0)	5°
Shape functions	12
System states	24

ent profiles: a linear case and a nonlinear case (see Figure 2). The nonlinear case (B) exhibits a static stall effect.

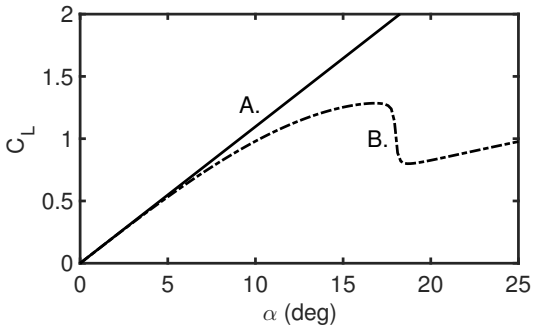

Figure 2: *C_L functions for linear (non-stall) and nonlinear (stall) cases. The nonlinear curve is fully stalled at $\alpha \approx 17°$.*

III. Results

Figure 3 shows a bifurcation diagram illustrating how the equilibrium position of the wing tip changes with velocity. It can be seen that the magnitude of steady state tip displacement increases as airspeed increases. In this first example, the linear C_L profile is used (Figure 2). Flutter is indicated by the occurance of a Hopf bifurcation at approximately 22.373 m/s; past this velocity the equilibria curve is unstable and thus the wing exhibits no stable static state. Figure 4 shows time histories for both below (V = 20 m/s) and above (V = 24 m/s) V_F, illustrating the presence of an LCO post-flutter. In the absence of stall effects, the existence of this LCO is exclusively due to the geometric nonlinearites (e.g. re-orientation of aerodynamic force vectors and effective tip shortening, see Figure 1) present in the system. If these nonlinearities were to be neglected, flutter in this case would comprise unbounded exponential growth. Figure 5 shows the spanwise wing deformation at V = 22 m/s; this steady deformation is relatively small, indicating that geometric nonlinearities are not largely influential in the flutter mechanism itself in this case.

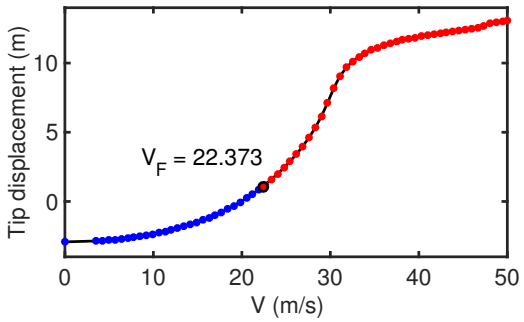

Figure 3: *Variation of steady state tip displacement with airspeed (linear C_L). Hopf bifurcation (V_F) occurs at 22.373 m/s. Blue and red curves indicate stable and unstable equilibria respectively.*

The nonlinear C_L function is now used. Figure 6 shows that the introduction of this lift profile increases the value of V_F to 23.247 m/s. This discrepancy is small because the wing is minimally twisted as it approaches the flutter condition; the combination of twist angle and α_0 is not sufficient for a large stalling influence. This can be seen in Figure 7; near the flutter point, the steady tip twist angle is $\approx 2°$, corresponding to an angle of attack $\approx 7°$ (since $\alpha_0 = 5°$). Figure 2 shows that stall effects are

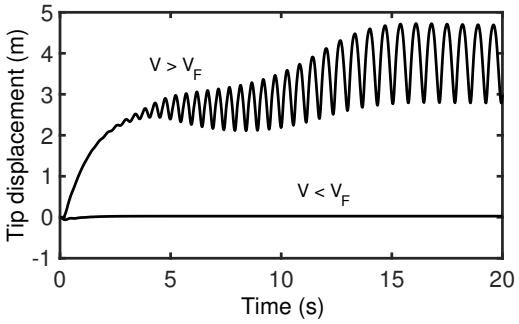

Figure 4: *Time histories for $V = 20\ m/s$ and $V = 25\ m/s$ (linear C_L), demonstrating behaviour before and after Hopf bifurcation.*

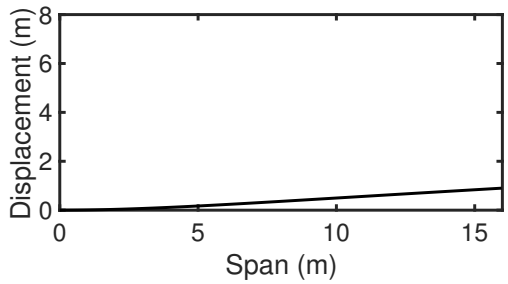

Figure 5: *Spanwise wing deformation at airspeed before flutter ($V = 22\ m/s$).*

relatively small at this angle. The influence of stall is more observable when considering post-flutter behaviour; Figure 8 shows that the LCO produced at the post-flutter velocity has a considerably smaller amplitude than that previously produced with the linear C_L profile (Figure 4). This discrepancy is explained when the corresponding tip twist time histories are compared (see Figure 9); the inclusion of the stall effect serves to significantly reduce the angles of attack achieved by the wing.

i. Effect of stiffness variation on V_F

The effect of varying the stiffness parameters about the nominal values shown in Table 1 is now considered. Figures 10, 11 and 12 illustrate how the value of V_F changes when the uncoupled stiffness properties of the wing are varied independently. Here, EI_1 corresponds to out-of-plane (flapwise) bending stiffness, EI_2 corresponds to in-plane (chord-wise) bending stiffness and GJ corresponds to torsional stiffness. In each case, stiffness is expressed as a % of the appropriate nominal value shown

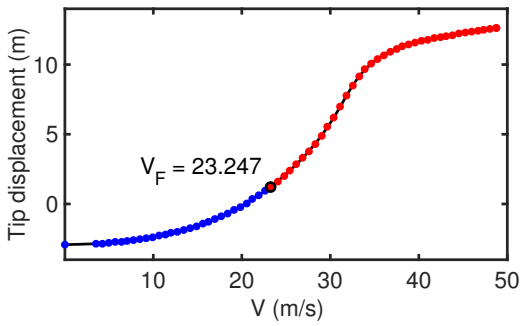

Figure 6: *Variation of steady state tip displacement with airspeed (nonlinear C_L). Hopf bifurcation (V_F) occurs at 23.247 m/s.*

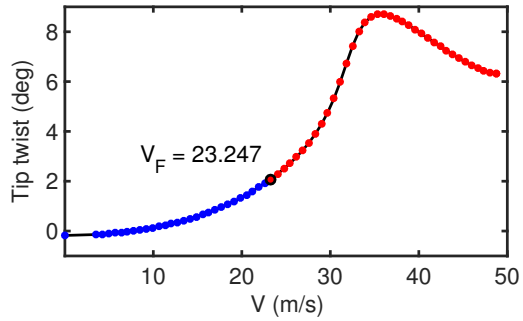

Figure 7: *Variation of steady state tip twst with airspeed (nonlinear C_L). Hopf bifurcation (V_F) occurs at 23.247 m/s.*

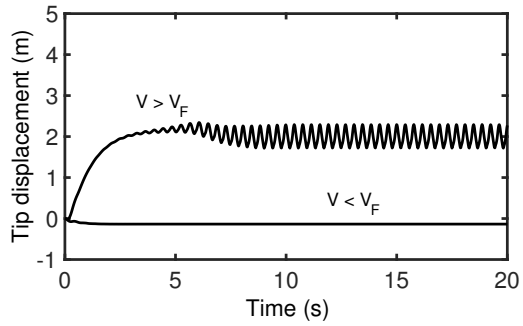

Figure 8: *Time histories for $V = 20\ m/s$ and $V = 25\ m/s$ (nonlinear C_L), demonstrating behaviour before and after Hopf bifurcation.*

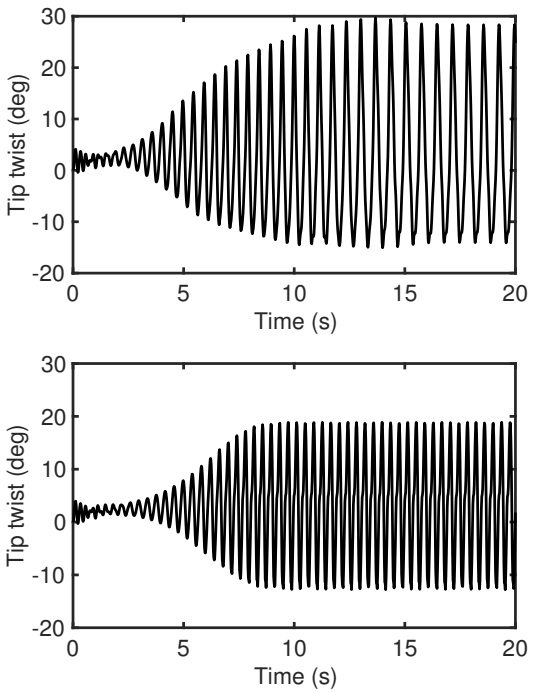

Figure 9: *Time histories for V = 25 m/s (linear C_L and nonlinear C_L respectively).*

in Table 1. Results produced using the linear C_L are represented by solid lines, whereas results produced using nonlinear C_L are represented by dashed lines. Since the value of V_F strictly corresponds to the lowest airspeed at which a Hopf bifurcation occurs, these figures do not correspond to smooth Hopf-point continuations which can display multiple solutions for ranges of stiffness values. This explains the apparent discontinuity in Figures 10 and 12.

It can be seen that in all cases, increasing stiffness increases V_F and the inclusion of the nonlinear C_L profile is beneficial in that it further delays V_F. It can be observed from Figure 11 that the variation of EI_2 has little influence. Figure 10 shows that varying EI_1 is similarly ineffectual, provided that it is above a threshold of $\approx 45\%$. Below this threshold, V_F drops off significantly as EI_1 is reduced. This drop-off is related to the inclusion of gravitational forces in the model; reduced EI_1 means that the wing is subject to significant downwards out-of-plane deformation due to self weight. Figure 13 illustrates the static spanwise wing deformation at stiffnesses below and above this threshold; the increased deformation observed at 30% is more favourable for the flutter mechanism. When gravitational effects are removed from the model, the rapid drop-off in V_F when reducing EI_1 is no longer present (see Figure 14). It can also be observed from this figure that removing gravity has a detrimental effect as a whole, as the

The influence of stall is most affected when GJ is varied, as shown by the discrepancy between the two curves in Figure 12. This is to be expected, as the variation of GJ directly relates to the angles of attack along the wing. There is a clear discrepancy between the linear and nonlinear (stall) results for values below $\approx 30\%$; here the torsional stiffness is sufficiently low so as to permit stalling angles of attack at low airspeeds.

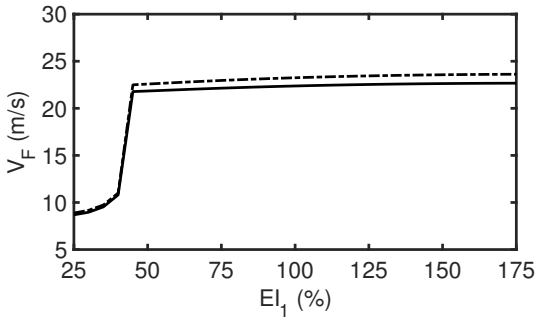

Figure 10: *Variation of flutter velocity with out-of-plane bending stiffness (solid = linear C_L , dashed = nonlinear C_L).*

Figure 15 illustrates the variation of V_F when EI_1 and GJ are varied simultaneously. This surface plot shows that the behaviour is generally dominated by the lowest stiffness parameter and that V_F remains low if the threshold identified from Figure 10 for EI_1 is not met (regardless of the the value of GJ).

ii. Subcritical LCOs

The Hopf bifurcation that occurs at the flutter velocity (V_F) may be one of two types; it may be subcritical or supercritical (see Figure 16).

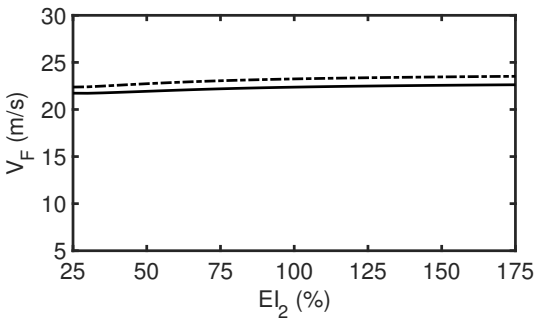

Figure 11: *Variation of flutter velocity with in-plane bending stiffness (solid = linear C_L , dashed = nonlinear C_L).*

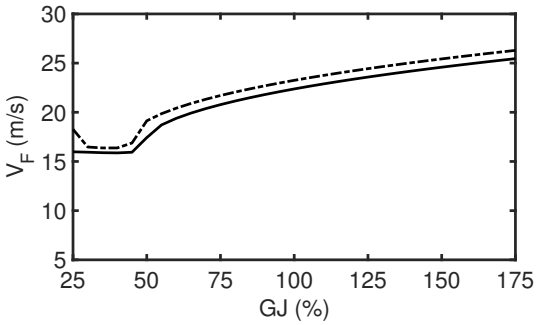

Figure 12: *Variation of flutter velocity with torsional stiffness (solid = linear C_L , dashed = nonlinear C_L).*

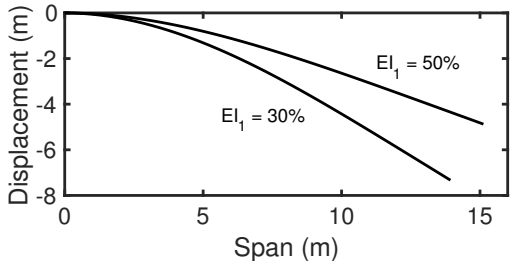

Figure 13: *Spanwise wing deformation at low airspeed ($V = 8$ m/s) for out-of-plane stiffness above and below threshold.*

In the supercritical case, the emanating limit cycle is stable and is only observable beyond the bifurcation point, i.e. at airspeeds that exceed V_F. The variation in system response is also reversible in that the oscillation can be removed smoothly by simply reducing the air-

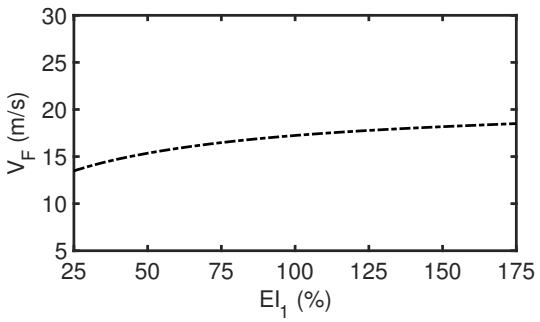

Figure 14: *Variation of V_F with EI_1 with gravitational effect excluded (linear C_L = solid, nonlinear C_L = dashed).*

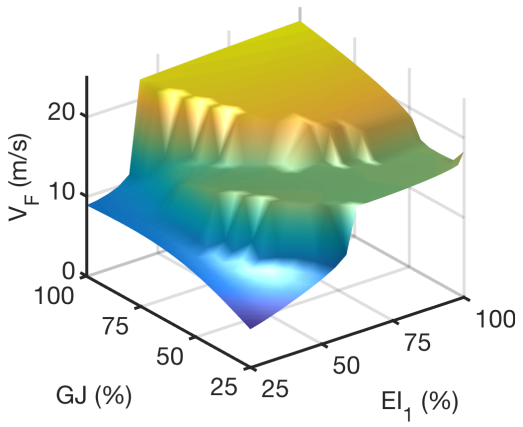

Figure 15: *Variation of flutter velocity with out-of-plane stiffness and torsional stiffness (nonlinear C_L).*

speed down to the bifurcation point. In the subcritical case, the limit cycle is unstable below the bifurcation point and typically folds back and changes stability; this gives rise to a hysteresis loop where the velocity must be reduced further than the bifurcation point to remove the LCO. At this point, the LCO would disappear suddenly as opposed to smoothly.

The occurrence of a subcritical Hopf bifurcation is significant in aeroelastic applications, as it essentially means that oscillatory behaviour is possible at airspeeds below the known flutter boundary (given a sufficient disturbance to the wing). Such a response is clearly undesirable for safety and fatigue reasons, so it follows that

determining the nature of the Hopf bifurcation is important. Tang and Dowell [6] and Patil et al. [7] observed subcritical behaviour in an experimental wind tunnel study and theoretical studies.

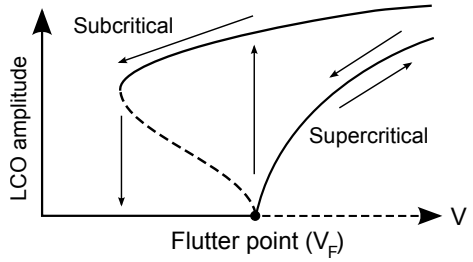

Figure 16: *Diagram showing LCO amplitude vs. velocity for the two generic Hopf bifurcations. Subcritical case shows LCO below V_F. Supercritical case is reversible whereas subcritical case exhibits hysteresis loop.*

With all nominal wing parameters restored (Table 1), numerical integration of the system reveals small LCOs at velocities slightly below V_F for both linear and nonlinear C_L, given a finite perturbation (the initial conditions are zero and thus the system is perturbed from the nonzero equilibrium). Figure 17 shows an example time history using nonlinear C_L for $V = 23.24$ (where $V_F = 23.247$). This result indicates that a subcritical Hopf occurs at the flutter point.

The numerical continuation technique used in the previous section is now modified so as to solve for periodic solutions. Figure 18 (upper) shows a trace of the maxima and minima of the limit cycle emanating from the bifurcation point as airspeed varies; this plot confirms the existence of the subcritical case as per Figure 16. Subcritical behaviour is similarly observed for the case where stall effects are excluded and the linear C_L is used (Figure 18, lower), thus confirming that the geometric nonlinearity alone is sufficient for the phenomenon in this case. In both diagrams, it is observed that the limit cycles undergo further bifurcations; these are not explored here.

For different wing parameters, the magnitude of this behaviour may vary. For example, different stiffness properties may exaggerate the subcritical nature of the Hopf bifurcation and may permit LCOs at airspeeds significantly lower than the bifurcation point. Conversely, there may be parameters that tailor the system to produce the more favourable supercritical case (see Figure 16), which typically only permits LCOs post-flutter. Investigation of these possibilities is the focus of ongoing work; the primary objective being to understand the fundamental mechanisms that determine the nature of the Hopf bifurcation.

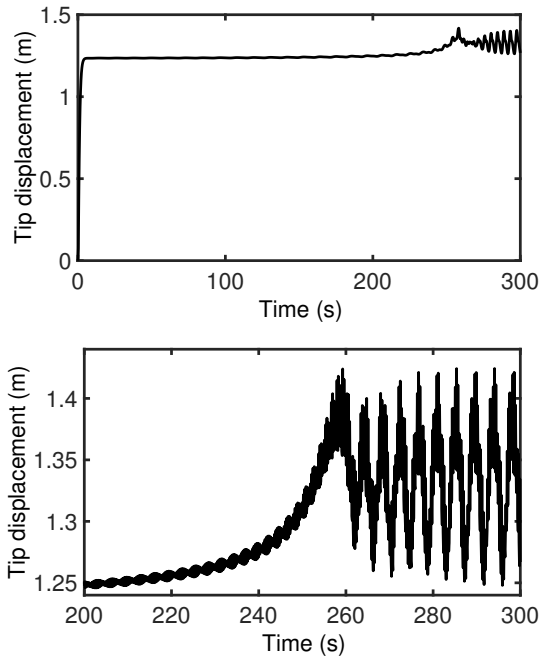

Figure 17: *Time history for $V = 23.24$ m/s (nonlinear C_L), showing LCO observable below the flutter velocity. This indicates the occurrence of a subcritical Hopf bifurcation. Note: the lower plot is a magnification of the upper plot.*

IV. Conclusions

This paper used numerical continuation techniques to investigate the occurrence of aeroelastic flutter in a high aspect ratio wing. Stiffness properties were varied about nominal values and it was observed that in-plane bending stiffness is not influential on the flutter speed. It

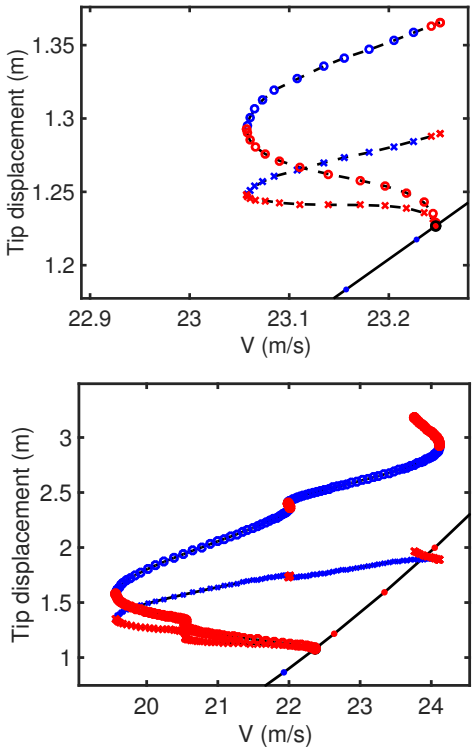

Figure 18: *Variation of steady state tip displacement with airspeed (nonlinear and linear C_L; upper and lower respectively), showing maxima (circle) and minima (cross) of periodic solution emanating from Hopf bifurcation. Presence of solution below V_F is indicative of subcritical behaviour in both cases.*

was found that out-of-plane bending stiffness is not important, provided that it is sufficient to prevent large deformation due to self weight. Torsional stiffness variation does have a notable influence on the onset of flutter. The inclusion of a static stall effect was observed to delay the onset of flutter in all cases when compared to a linear lift profile. Subcritical behaviour was identified using both numerical integration and continuation and therefore warrants further study in this area.

V. Acknowledgements

This research is funded by the Airbus InnovateUK Agile Wing Integration Project (TSB-113041). Simon Neild is supported by an EPSRC fellowship (EP/K005375/1) and Jonathan Cooper holds a Royal Academy of Engineering Research Chair.

References

[1] M.K. Bradley and C.K. Droney (2012). "Subsonic ultra green aircraft research phase II: N+ 4 advanced concept development". *NASA/CR-2012-217556*.

[2] C. Howcroft, R. Cook, D. Calderon, L. Lambert, M. Castellani, J.E. Cooper, M. Lowenberg, S.A. Neild and E. Coetzee (2016). "Aeroelastic Modelling of Highly Flexible Wings". *AIAA SciTech Conference*, 2016-1798.

[3] E. Dowell, J. Edwards and T. Strganac (2003) "Nonlinear Aeroelasticity" *Journal of Aircraft*, 40(5):857-874.

[4] C. Howcroft, S.A. Neild, M.H. Lowenberg, J.E. Cooper (2016). "Aeroelastic Modelling of Highly Flexible Wings". *USD2012 International Conference on Uncertainty in Structural Dynamics*, (to appear in proceedings of) , Leuven, Belgium, 19-21 September, (2016).

[5] M.J. Patil, D.H. Hodges and C.E.S. Cesnik (2001). "Nonlinear Aeroelasticity and Flight Dynamics of High-Altitude Long-Endurance Aircraft". *Journal of Aircraft*, 38(1):88-94.

[6] D.M. Tang and E. Dowell (2001) "Experimental and Theoretical Study on Aeroelastic Response of High-Aspect-Ratio Wings". *AIAA Journal*, 39(8):1430-1441.

[7] M.J. Patil, D.H. Hodges and C.E.S. Cesnik (2001). "Limit Cycle Oscillations in High-Aspect-Ratio Wings". *Journal of Fluids and Structures*, 15:107-132.

[8] S. Sharma, E.B. Coetzee, M.H. Lowenberg, S.A. Neild, B. Krauskopf (2015) "Numerical continuation and bifurcation analysis

in aircraft design: an industrial perspective." *Philosophical Transactions of The Royal Society A: Mathematical, Physical and Engineering Sciences*, Vol: 373 Issue: 2051.